ACS Catalysis

Research Article

pubs.acs.org/acscatalysis

Reactivity and Regioselectivity of Methylacetylene Cyclotrimerization over the Phillips Cr/Silica Catalyst: A DFT Study

Zhen Liu, Ruihua Cheng, Xuelian He, and Boping Liu*

State Key Laboratory of Chemical Engineering, East China University of Science and Technology, 130 Meilong Road, 200237, Shanghai, China

Supporting Information

ABSTRACT: The mechanism of the methylacetylene cyclotrimerization catalyzed by the Phillips Cr/silica catalyst has been studied by DFT investigations based on a Cr(II)/SiO_2 cluster model and a silica supported cluster model. Twenty-one kinds of Cr(II)/SiO_2·$(C_3H_4)_n$ (n = 1−3) complexes were first optimized successfully. Starting from the most stable chromium(methylacetylene) complex, the following cyclotrimerization of methylacetylene on the quintet surface is prohibited by the spontaneous coupling of the two coordinated methylacetylenes. Instead of overcoming a much higher Gibbs free energy barrier by about 40 kcal/mol on the quintet surface, a spin flipping to the triplet surface at the chromium(methylacetylene) complex only requires 16.9 kcal/mol in Gibbs free energy. After the spin transition, the methyl-chromacyclopropene species was formed immediately on the triplet surface. The triplet dimethyl-chromacyclopentadiene species was generated by insertion of a coordinated methylacetylene into the 3-membered metallacycle ring. The following reaction may follow two pathways: (a) a concerted [4 + 2] cycloaddition or (b) a stepwise pathway (insertion and reductive elimination) via a trimethyl-chromacycloheptatriene species. All the eight [4 + 2] cycloaddition reaction pathways are favored competing with the stepwise pathways. The reactivity of each reaction pathway can be examined in terms of the calculated TOF using the energetic span model. We found that only four [4 + 2] cycloaddition reaction pathways (PES-T1Da, PES-T2Da, PES-T3Da, and PES-T4Da) are responsible for the cyclotrimerization of methylacetylene. The PES-T4Da leads to the production of 1,3,5-trimethylbenzene, while the other three pathways generate 1,2,4-trimethylbenzene. Furthermore, the effects of the silica support and the dispersion correction have been considered for the most plausible reaction pathways PES-T1Da, PES-T2Da, PES-T3Da, and PES-T4Da, respectively. Finally, with a consideration of the effects of the silica support and inclusion of the dispersion correction in the final calculated energies, the ratio of the 1,3,5- to 1,2,4-TMB is 0.32 at 363 K predicting that the 1,2,4-TMB is the dominant product in the cyclotrimerization of methylacetylene catalyzed by the Phillips Cr/silica catalyst.

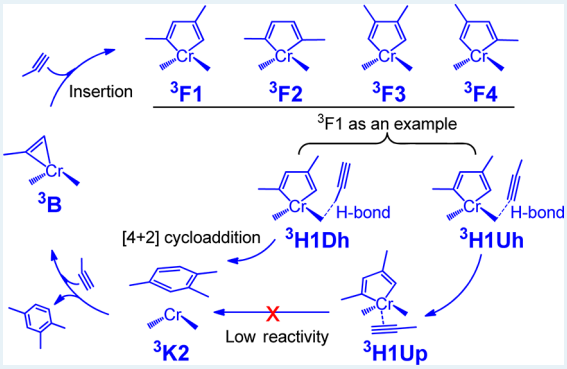

KEYWORDS: *methylacetylene cyclotrimerization, Phillips chromium catalyst, DFT, TOF, spin flipping*

1. INTRODUCTION

The Phillips Cr/silica catalyst was first discovered in the last half of 1951 by J. P. Hogan and R. L. Banks from the Phillips Petroleum Company.[1] Soon after the great invention, the Phillips Company filed two important patents on olefin polymerization[2] and alkyne cyclotrimerization[3] catalyzed by the Phillips Cr/silica catalyst. After a long period of development, nowadays, more than one-third of world industrial high-density polyethylene is produced using the Phillips Cr/silica catalyst.[1]

During the past 60 years, Phillips Cr/silica catalyst has been attracting tremendous research efforts in both the industrial and academic fields in order to elucidate the structures of the active sites, the oxidation states of the chromium center, and the mechanisms for ethylene polymerization.[1,4] Although many spectroscopic investigations had been conducted on the Phillips Cr/silica catalyst, the precise structure of the active site is still obscure without the assistance of the theoretical calculations.[4] Espelid and Børve had performed a series of density functional theory (DFT) studies on the Phillips Cr/silica catalyst with a comparison to the spectroscopic observations and found that a six-membered chromasiloxane(II) ring is the most reasonable model of silica-anchored chromium active site.[5−7] The six-membered chromasiloxane(II) ring was soon supported by Scott et al. on the basis of their experimental and theoretical studies.[8] Thenceforth, the six-membered chromasiloxane(II) ring has been employed as a cluster model for the Phillips Cr/silica catalyst.[9−14]

Unlike the tremendous research conducted on the chromium catalyzed ethylene polymerization, study on the cyclotrimeriza-

Received: September 29, 2012
Revised: April 3, 2013
Published: April 8, 2013

tion of the short alkynes is surprisingly rare.[1] Only two reports on the cyclotrimerization of alkynes catalyzed by the Phillips Cr/silica catalyst were published elsewhere.[15,16] The first report came from the Phillips Petroleum Company as well, which is only a year later after they patented the alkyne cyclotrimerization catalyzed by the Phillips Cr/silica catalyst.[15] In their report, the acetylene was found primarily cyclotrimerized into benzene, while a ratio of 0.18 of 1,3,5- to 1,2,4-trimethylbenzene (TMB) was obtained for the methylacetylene cyclotrimerization.[15] They gave an explanation on the ratio of 0.18 as stated in the paper: "Statistically, there are 5 ways in which three propyne molecules can be grouped to form 1,2,4-trimethylbenzene, and only one way to form 1,3,5-trimethylbenzene. From this approach, one would expect, if there were no special directive influences, a ratio of 1,3,5- to 1,2,4-trimethylbenzene of 1/5 =0.20, which is very close to the actual ratio of 0.18. This could be considered an evidence of little or no directive influence in the cyclic joining of three propyne molecules. There would be a great deal of scientific value in a further study of this problem." In the other experimental report, however, the cyclotrimerization of methylacetylene was found to yield a pure cyclic product of 1,3,5-TMB.[16] Subsequently, two questions are raised from these two experiments: (a) How many reaction pathways are there in which three methylacetylene molecules can be grouped into a cyclic product? (b) What is the expected ratio of 1,3,5- to 1,2,4-TMB?

Indebted to theoretical calculations, the mechanisms of acetylene cyclotrimerization catalyzed by various transition metals have been clearly elucidated during the past decade.[17−32] The acetylene cyclotrimerization catalyzed by the Phillips Cr/silica catalyst was reported by us very recently.[12] In our previous study of acetylene cyclotrimerization, two contributions were achieved: with an extensive benchmark test, a suitable DFT functional was recognized for the description of the Cr(II)/SiO_2 cluster model, and more importantly, the spin crossover phenomenon was observed for the acetylene cyclotrimerization catalyzed by the Cr(II)/SiO_2 cluster model. In this study, we are trying to unravel the mechanisms for chromium catalyzed methylacetylene cyclotrimerization with a consideration of the reactivity and regioselectivity. All the possible reaction pathways for methylacetylene cyclotrimerization have been fully explored on two possible potential energy surfaces using a carefully benchmarked DFT method. Moreover, all the Gibbs free energy profiles for each of the reaction pathways on the quintet and triplet surfaces are presented. To examine the feasibility of these reaction pathways, the energetic span model developed by Kozuch and Shaik was employed for calculating the turnover frequency (TOF) of each catalytic cycle.[33−35] Basically, the energetic span model bridges the gap between theory and experiment in catalysis and allows us to predict the efficiency of the catalytic cycle in terms of its TOF.[36,37]

This work is a continuous investigation on the chromium catalyzed alkyne cyclotrimerization. The findings of our previous computational study on acetylene cyclotrimerization catalyzed by the Phillips Cr/silica catalyst was first summarized and compared with another possible single-state reaction mechanism. Due to the unsymmetrical nature of the methylacetylene molecule, the reaction mechanism of the cyclotrimerization is far more sophisticated than that of the acetylene cyclotrimerization. To the best of our knowledge, this is the first detailed theoretical study on the mechanism of methylacetylene cyclotrimerization.

2. A REVISIT OF ACETYLENE CYCLOTRIMERIZATION CATALYZED BY THE PHILLIPS CR/SILICA CATALYST: A TWO-STATE REACTIVITY VS A SINGLE-STATE REACTIVITY

Very recently, we reported a theoretical investigation on the cyclotrimerization of acetylene by the Cr(II)/SiO_2 model catalyst.[12] The ground spin states of chromium(acetylene) adducts are known to be of quintet, and the most plausible reaction pathway on the quintet surface needs to overcome two activation barriers to complete one turn of the catalytic cycle. The free-energy barrier for the rate-determining step is computed to 31.1 kcal/mol, leading to a turnover frequency of 1.36×10^{-9} h^{-1} and effectively ruling out the quintet mechanism for acetylene cyclotrimerization by the Cr(II)/SiO_2 model catalyst. Details are provided in ref 12.

In our previous work,[12] the proposed two-state mechanism following the pathway ^{5}**I** → ^{5}**II** → $^{5-3}$**CPI** → ^{3}**II** → ^{3}**III** → ^{3}**V** → ^{3}**VI** → ^{3}**VII** → $^{5-3}$**CPII** → ^{5}**VII** → ^{5}**I′** for acetylene cyclotrimerization requires two spin-inversion processes, as

Scheme 1. Two Proposed Mechanisms for Acetylene Cyclotrimerization by Cr(II)/SiO_2 Cluster Model: A Two-State Reactivity vs a Triplet Catalytic Cycle

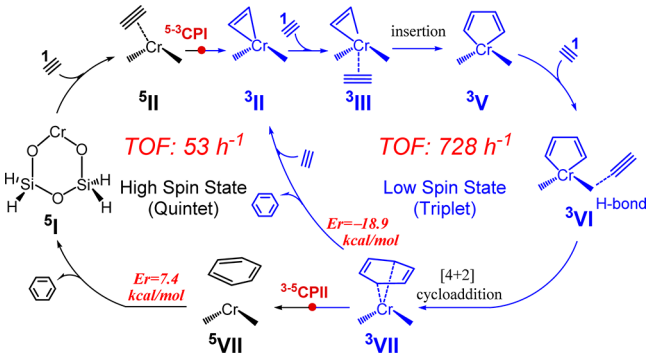

depicted in Scheme 1. The first minimum energy crossing point $^{5-3}$**CPI** is crucial for initiation of acetylene cyclotrimerization. In this regard, the insertion of a second acetylene molecule into a 3-membered ring on the triplet surface was found to be much more facile than that proceeding through oxidative coupling on the quintet surface. Rather than crossover to the quintet surface through $^{3-5}$**CPII**, the displacement of benzene ring by acetylene on the triplet surface was predicted to be thermodynamically favorable with an exergonicity of 18.9 kcal/mol. The calculated TOF for the above-mentioned two-state catalytic cycle is about 53 h^{-1}, which is much lower than the TOF of 728 h^{-1} for the newly suggested reaction pathway on a single triplet surface. Therefore, the acetylene cyclotrimerization by the Cr(II)/silica model catalyst initiates with coordination of an acetylene molecule on the quintet surface. After a spin-flipping at the quintet chromium(acetylene) complex, the following catalytic cycle favors a triplet [4 + 2] cycloaddition pathway.

3. COMPUTATIONAL DETAILS

In order to extensively explore the reaction pathways of the methylacetylene cyclotrimerization, we first use a six-membered chromasiloxane(II) ring (model A, as shown in Figure 1) as a model of the active site for the Phillips Cr/silica catalyst. The chromium(methylacetylene)$_x$ adducts were first studied, and then the mechanisms for methylacetylene cyclotrimerization

dx.doi.org/10.1021/cs400129g | ACS Catal. 2013, 3, 1172−1183

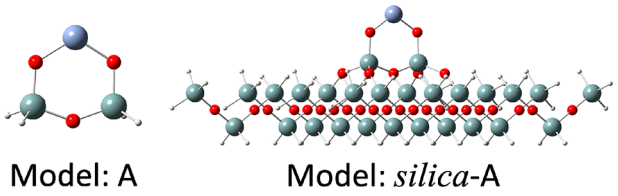

Figure 1. A six-membered chromasiloxane(II) cluster model A and a silica supported cluster model *silica*-A.

were fully investigated with consideration of the spin-crossover phenomenon. Finally, the most plausible reaction pathways for methylacetylene cyclotrimerization were recognized. Due to the omission of the silica surface in the six-membered chromasiloxane(II) ring, theoretical calculations based on the small size of the clusters may introduce artificial effects.[38] In our recent study,[13] a silica-supported cluster model was built by anchoring the six-membered chromasiloxane(II) ring on the fully dehydroxylated (100) β-cristobalite surface for modeling the active site of the Phillips Cr/silica catalyst. The similarity of amorphous silica surface and β-cristobalite was experimentally reported,[39−42] and many theoretical simulations of amorphous silica are also based on the β-cristobalite structure.[13,43−51] Therefore, we further calculated the most plausible reaction pathways for methylacetylene cyclotrimerization using a large silica supported cluster model containing 30 Si atoms referred to as model *silica*-A as shown in Figure 1.

All geometry optimizations, frequency calculations, and full intrinsic reaction coordinate (IRC) calculations were performed in Gaussian09.[52] The hybrid DFT functional B3PW91′ (28% Hartree−Fock exact exchange energy) with a basis set of triple-ξ quality was applied for all the calculations. That is, the chromium atom was described by a triple-ξ basis set with the effective core potential of Hay and Wadt (LANL2TZ(f)), and the full electron Pople's basis set 6-311G(d,p) was used for the other elements. The selected DFT functional and the basis sets have already been benchmarked for the description of the Cr(II)/SiO_2 cluster model in our previous study.[12] From our previous benchmark test, the hybrid DFT functional B3PW91′ gave a good description of the triplet−quintet energy gap of the cluster model Cr(II)/SiO_2. We then calculated the enthalpy and Gibbs free energy of the formation of 1,2,4-TMB and 1,3,5-TMB, respectively. The calculated values are in good agreement with the standard enthalpies and the Gibbs free energies of formation, as listed in Table 1. Therefore, the B3PW91′ with a basis set of the triple-ξ quality is qualified for the mechanistic study on the cyclotrimerization of methylacetylene catalyzed by the Cr(II)/SiO_2 cluster model. Throughout, we have employed harmonic vibrational frequency calculations to confirm that structures have been properly optimized. The transition state was further verified by a full IRC calculation, which showed a direct connection between the corresponding reactant and the product. A larger DFT integration grid (keyword: int = ultrafine) was used for all the DFT calculations in order to obtain more reliable results. The methodology developed by Harvey[53,54] and co-workers was employed to locate the minimum energy crossing point (MECP) between two adjacent potential energy surfaces. The quadratic convergence SCF method (keyword: scf = xqc) was employed whenever the SCF failed to converge. Originally, the Gibbs free energies were computed at 298.15 K and 1 atm as default for all the stationary points on each of the potential energy surfaces, while the free energy corrections at the MECPs were estimated with the freq = projected keyword available in Gaussian09. We further evaluate the Gibbs free energies for the species on the most plausible reaction pathways at another two different conditions (250 K, 1 atm and 363 K, 40.8 atm) in order to compare our calculation results with the corresponding experimental reports in the literature. The TOF of each reaction pathway was predicted using the energetic span model and calculated with a user-friendly AUTOF program, which were recently developed by Kozuch and Shaik.[33−35] In the calculations with the *silica*-A cluster model, the silica surface part including 122 atoms was kept frozen during the geometry optimization. The same basis set (LANL2TZ(f) for Cr, 6-311G(d,p) for Si, O, C, H) was also employed for the calculations when using the *silica*-A cluster model. We further analyzed the effect of the inclusion of Grimme's dispersion corrections[55] for the most plausible reaction pathways and calculated the corresponding TOFs for each pathway using the corrected energy profiles. The dispersion corrections were calculated using the DFT-D3 (zero-damping) code developed by Grimme and co-workers recently.[56]

Table 1. The Enthalpy and Gibbs Free Energy of the Reaction[a] for the Cyclotrimerization of Methylacetylene into TMB

	ΔH	ΔH^0	ΔG	ΔG^0
1,2,4-TMB	−135.4	−136.5	−111.5	−111.6
1,3,5-TMB	−136.0	−137.0	−113.9	−111.4

[a] ΔH^0 and ΔG^0 are the standard enthalpy and Gibbs free energy of the reaction. (The source data is taken from http://www.chemeo.com). ΔH and ΔG are the calculated enthalpy and Gibbs free energy of the reaction at 298.15 K and 1 atm. Energies are in kcal/mol.

4. RESULTS AND DISCUSSION

We first present all the possible chromium(methylacetylene) adducts in the ground spin state with up to three methylacetylenes adsorbed on the cluster model A. In the following mechanistic study, two competitive mechanisms (a concerted [4 + 2] cycloaddition and a stepwise pathway via insertion and reductive elimination) are taken into consideration. On each of the quintet and triplet surfaces, all the possible reaction pathways are explored extensively using full IRC calculations. The reactivity and regioselectivity of these pathways are discussed and compared in terms of the calculated turnover frequency values.

4.1. Chromium(Methylacetylene) Adducts. In our previous study, four kinds of Cr(II)/SiO_2·$(C_2H_2)_n$ (n = 1−3) adducts were located through DFT calculations.[12] The coordination of methylacetylene on the chromium center is much more complicated comparing with the adsorption of acetylene molecules. The frontier orbitals of acetylene and methylacetylene and the NBO charges for each atom in these two molecules are shown in Figure 2. The $\sigma-\pi$ hyperconjugation (HOMO−2) induced by the methyl group in methylacetylene enhances the electron density at C1 at the expense of C2. Thus, the methyl group may act as hydrogen-bonding donor when adsorbing on the chromium active center resulting in a slightly stronger hydrogen bond.

Table 2 lists binding Gibbs free energies for all the Cr(II)/SiO_2·$(C_3H_4)_n$ (n = 1−3) adducts. The optimized geometrical features of Cr(II)/SiO_2·$(C_3H_4)_n$ (n = 1−2) complexes are shown in Figure 3, while the Cr(II)/SiO_2·$(C_3H_4)_3$ complexes

dx.doi.org/10.1021/cs400129g | ACS Catal. 2013, 3, 1172−1183

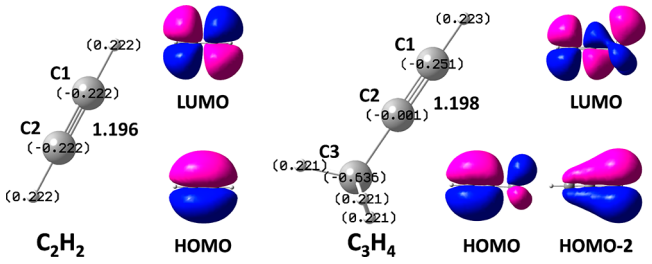

Figure 2. Frontier orbitals and NBO analysis of acetylene and methylacetylene. (0.02 au$^{-3/2}$ isovalue).

Table 2. The Binding Gibbs Free Energies[a] for the Cr(II)/SiO_2·$(C_3H_4)_n$ (n = 1−3) Adducts

	$^5\Delta G$		$^5\Delta G$		$^5\Delta G$
^{5}B1	−7.0	^{5}C1/^{5}C4	−3.4	^{5}D1	3.3
				^{5}D2	4.1
				^{5}D3	2.0
				^{5}D4	2.8
				^{5}D5	2.5
				^{5}D6	2.2
				^{5}D7	1.4
				^{5}D8	*b*
		^{5}C2	−4.5	^{5}D9	1.6
				^{5}D10	1.8
				^{5}D11	1.0
				^{5}D12	1.1
^{5}B2	−5.1	^{5}C3	−2.4	^{5}D13	3.2
				^{5}D14	3.9
				^{5}D15	2.1
				^{5}D16	3.4

[a]ΔG is the binding Gibbs free energy relative to the corresponding free methylacetylenes and the quintet-state Cr(II)/SiO_2 cluster model at 298.15 K and 1 atm. [b]The geometry optimization of ^{5}**D8** is converged to the same geometry of ^{5}**D12**. The superscript digit denotes the spin multiplicity. Energies are in kcal/mol.

are depicted in Figure S1 in the Supporting Information. The Cr(II)/SiO_2 cluster model ^{5}**A** (the superscript number denotes the spin multiplicity of the species) prefers a quintet ground spin state and exhibits a C_{2v} symmetry as calculated in our previous study.[12] Unlike the acetylene molecule, the methylacetylene molecule is unsymmetrical and always has two different orientations for its interaction with the cluster model. Two kinds of π-complexes ^{5}**B1** and ^{5}**B2** could be generated through the coordination of the first methylacetylene molecule on the chromium center in a methyl-group-down (MG-down) orientation and in a methyl-group-up (MG-up) orientation, respectively. The π-complexes ^{5}**B1** and ^{5}**B2** were further stabilized through the formation of a hydrogen bond between a terminal hydrogen atom in methylacetylene molecule and an oxygen atom from the −Si−O−Cr− in the cluster model. In complex ^{5}**B1**, a stronger hydrogen bond with a shorter H−$O_{(1)}$ bond length of 2.204 Å was formed than that of 2.433 Å in ^{5}**B2** resulting in a more stable complex ^{5}**B1** by 1.9 kcal/mol. The orientation of the methyl group is crucial for such energetic difference between the π-complexes ^{5}**B1** and ^{5}**B2**.

Starting from ^{5}**B1**, ^{5}**C1** was generated by further coordination of a second methylacetylene molecule in a MG-up orientation, while ^{5}**C2** was yielded by coordinating a second methylacetylene in a MG-down orientation. Similarly, the bis(methylacetylene)-chromium complexes ^{5}**C3** and ^{5}**C4** were formed by coordination of a second methylacetylene molecule on ^{5}**B2** in MG-up and MG-down orientations, respectively. ^{5}**C1** and ^{5}**C4** exhibit the same geometrical features with a binding Gibbs free energy of −3.4 kcal/mol. With the formation of two strong hydrogen bonds of about 2.292 Å, ^{5}**C2** is the most stable bis(methylacetylene)−chromium complex and exhibits a C_2 symmetry. Similarly, ^{5}**C3** is also C_2 symmetric with two methylacetylene molecules coordinated in a MG-up orientation. However, ^{5}**C3** is predicted to be the least stable complex because of the formation of two weak hydrogen bonds of about 2.550 Å. All four bis(methylacetylene)−chromium adducts are predicted to be stable at room temperature as indicated by the binding Gibbs free energies as shown in Table 2. A third methylacetylene molecule could only be adsorbed on the cluster model through the formation of a hydrogen bond without any interaction with the chromium center. Since ^{5}**C1** is a complex without any symmetry, statistically, eight tri(methylacetylene)−chromium complexes could be generated by adsorbing a third methylacetylene molecule in both MG-down and MG-up orientations at the position of two oxygen atoms within the −Si−O−Cr−O−Si− from the front and back sides of the cluster model plane. However, the complex ^{5}**C1** turned into ^{5}**C2** while the third methylacetylene molecule in a MG-up orientation approaches to the left oxygen atom $O_{(1)}$ from the back side. Therefore, the tri(methylacetylene)−chromium complex ^{5}**D8** is not stable and turned into ^{5}**D12** during the geometry optimization. The adsorption of the third methylacetylene molecule on ^{5}**C4** is the same process as takes place on ^{5}**C1**. Only four tri(methylacetylene)−chromium complexes could be generated through coordination of a third methylacetylene on ^{5}**C2** or ^{5}**C3**, because the front and back sides are sterically identical for a complex with a C_2 symmetry. In total, fifteen tri(methylacetylene)−chromium complexes have been successfully optimized, and the geometrical features are depicted in Figure S1 in the Supporting Information. The binding Gibbs free energies for all fifteen complexes are positive, indicating that the third methylacetylene molecule could not be stably adsorbed only through the formation of a hydrogen bond with the cluster model. This finding rules out the formation of the cyclic product in a single step through a concerted [2 + 2 + 2] cycloaddition proposed by Zecchina et al.[16]

In summary, the Cr(II)/SiO_2 cluster model is able to stably coordinate up to two methylacetylene molecules yielding two kinds of mono(methylacetylene)−chromium complexes (^{5}**B1** and ^{5}**B2**) and four kinds of bis(methylacetylene)−chromium complexes (^{5}**C1**, ^{5}**C2**, ^{5}**C3**, and ^{5}**C4**). The following cyclotrimerization reaction may start from ^{5}**B**s because they are the most stable complexes and thus should be formed in abundance.

4.2. Quintet Pathways for Methylacetylene Cyclotrimerization. As discussed in the previous section, four kinds of bis(methylacetylene)−chromium complexes have been successfully optimized. Although ^{5}**C1** and ^{5}**C4** have the same geometrical features, the subsequent oxidative coupling generates two different kinds of dimethyl-chromacyclopentadiene species, ^{5}**F1** and ^{5}**F4**, respectively. Therefore, four different isomers of ^{5}**F** could be generated (^{5}**F1**, 1,3-dimethyl-chromacyclopentadiene; ^{5}**F2**, 1,4-dimethyl-chromacyclopentadiene; ^{5}**F3**, 2,3-dimethyl-chromacyclopentadiene; ^{5}**F4**, 2,4-dimethyl-chromacyclopentadiene), as drawn in Scheme 2. Depending on the orientation of the third methylacetylene

dx.doi.org/10.1021/cs400129g | ACS Catal. 2013, 3, 1172−1183

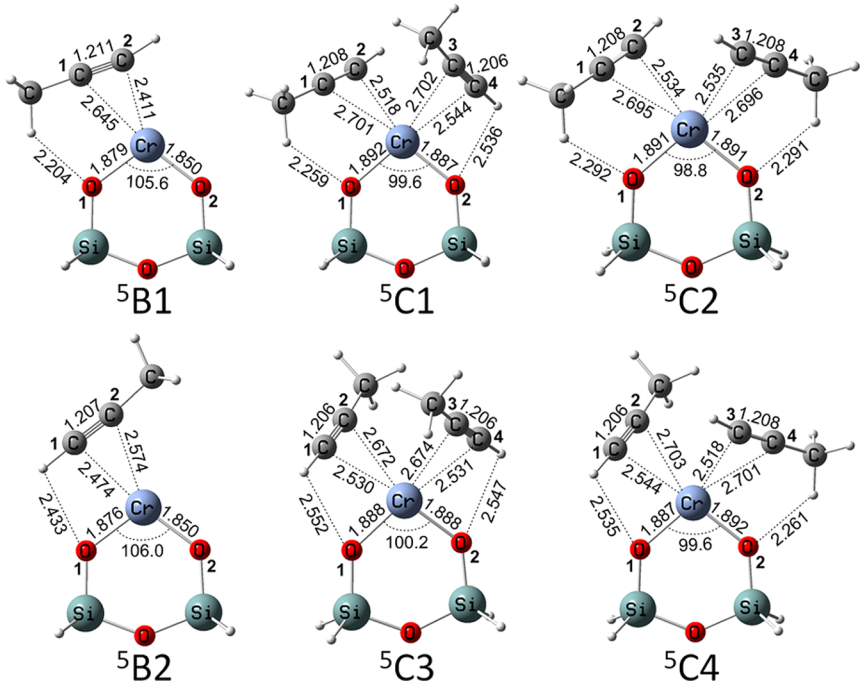

Figure 3. Optimized geometries of the quintet Cr(II)/SiO_2·$(C_3H_4)_n$ (n = 1−2) adducts. Bond lengths are in angstroms. Angles are in degrees.

Scheme 2. The Plausible Paths for the Cyclotrimerization of Methylacetylene on the Quintet Surface

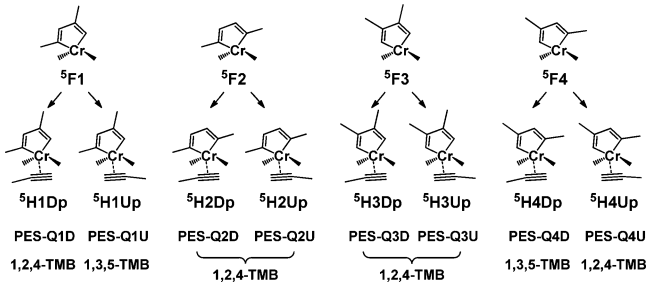

molecule, 22 isomers of ^{5}**H** were obtained. For instance, a kind of a hydrogen-bonded complex ^{5}**H1Dh** (h indicating the interaction of a third methylacetylene only through a hydrogen bond) was formed by adsorbing a third methylacetylene molecule on ^{5}**F1** in a MG-down orientation from the back side of the cluster model. On the other hand, two kinds of π-complexes ^{5}**H1Dp** (p indicating the interaction of a third methylacetylene mainly through pi-coordination) and ^{5}**H1Dp′** could be generated through coordination of a methylacetylene in MG-down orientation in the front side of the cluster model. In the same manner, the third methylacetylene molecule adsorbed on ^{5}**F1** in a MG-up orientation yields another two complexes (^{5}**H1Uh** or ^{5}**H1Up**). As shown in Scheme 2, there are six paths leading to the production of 1,2,4-TMB, while the other two paths yield 1,3,5-TMB. The reaction may proceed with [4 + 2] cycloaddition or a stepwise (insertion and reductive elimination) pathway, which gives 16 reaction pathways in total. The reaction pathway PES-Q1D is discussed in great detail in the Supporting Information (Scheme S1 and Figures S2−S4), and the relative Gibbs free energies for all the intermediates on the 16 quintet pathways are given in Scheme S2 in the Supporting Information.

Similar to acetylene cyclotrimerization, the rate-determining transition state on the quintet surface is the first activation barrier that transforms two coordinated methylacetylenes into a metallacycle ring. Therefore, the reactivity and regioselectivity of the methylacetylene cyclotrimerization on the quintet surface is primarily determined by the first activation barrier $^5\Delta G_1^{\ddagger}$(**B-E**), leaving the barrier $^5\Delta G_2^{\ddagger}$(**F-K**)/$^5\Delta G_2^{\ddagger}$(**F-I**) in a second place. The calculated TOFs for all the pathways on the quintet surface are extremely small as shown in Table S1 in the Supporting Information, which disagrees with the experimental observations.[15,16] Thus, the reaction pathways on a single quintet surface could be excluded for the methylacetylene cyclotrimerization reaction.

4.3. Spin Transition from Quintet to Triplet Surface.

Each quintet reaction pathway for methylacetylene cyclotrimerization needs to overcome a much higher Gibbs free energy barrier leading to a very low TOF for the catalytic cycle. Our previous study on the acetylene cyclotrimerization showed that some of the intermediates along the reaction pathway exhibit a triplet ground spin state.[12] We carefully calculated all the singlet and triplet geometries corresponding to the structures on the quintet surface. The reaction pathways on each of the singlet and triplet surfaces were also explored using full IRC calculations. The relative Gibbs free energies for the key intermediates along the reaction pathways on the three possible potential energy surfaces (singlet, triplet, and quintet) are shown in Figure S5 in the Supporting Information. The species **A**, **B**, and **C** exhibit a quintet ground spin state, while the key intermediates **F** and **H** favor a triplet ground spin state. The singlet species lie much higher in Gibbs free energy and thus are not discussed here. Therefore, a spin transition from the quintet surface to the triplet surface is highly expected. The triplet reaction pathway may give rise to reactivity that differs from that of its quintet analogue.

As observed in chromium catalyzed alkene dimerization[57] and trimerization reaction,[58] the spin crossover always facilitates the reaction and gives a raised reactivity for the catalytic cycle on the low spin surface. Before we discuss the reaction mechanisms on the triplet surface, we have to check

dx.doi.org/10.1021/cs400129g | ACS Catal. 2013, 3, 1172−1183

the possibility of the spin transition for the chromium-(methylacetylene) adduct from its quintet ground spin state to an adjacent triplet potential energy surface. The spin crossover may take place directly at the cluster model or at the chromium(methylacetylene) adduct. In order to find an MECP with the lowest energy, three MECPs ($^{5-3}$**CP1**, $^{5-3}$**CP2**, and $^{5-3}$**CP3**) were located at the cluster model and the most stable adducts with one or two π-coordinated methylacetylenes (^{5}**B1** and ^{5}**C2**), respectively. As shown in Figure 4, the spin transition

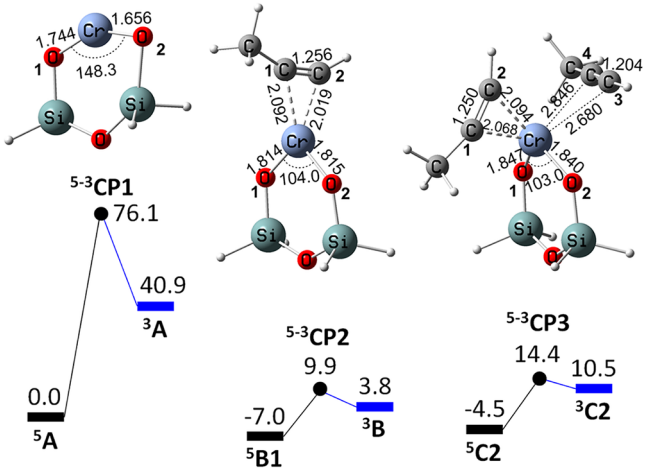

Figure 4. Gibbs free energy profile at 298.15 K for the spin crossover at ^{5}**A**, ^{5}**B1**, and ^{5}**C2**. The quintet parts are shown in black, while the triplet complexes are in blue. The MECPs are marked with a solid circle. Energies are in kcal/mol and relative to ^{5}**A** plus the corresponding number of methylacetylenes.

directly to the cluster model is prohibited by presenting an MECP $^{5-3}$**CP1**, which lies 76.1 kcal/mol higher in Gibbs free energy above ^{5}**A**. In $^{5-3}$**CP1**, the cluster model showed a distorted geometry and the oxygen atom $O_{(2)}$ was almost extruded from the six-membered ring, which raised the energy of the MECP $^{5-3}$**CP1** enormously. With coordination of the methylacetylene molecules, the spin flipping at ^{5}**B1** to its triplet analogous ^{3}**B** only requires Gibbs free energy of 16.9 kcal/mol, while the spin transition between ^{5}**C2** and ^{3}**C2** requires a slightly higher Gibbs free energy of 18.9 kcal/mol. Therefore, the spin flipping is predicted to be occurring at the most stable complex ^{5}**B1** through an MECP $^{5-3}$**CP2**. After this transition, a raised reactivity for the catalytic cycle on the triplet surface is highly expected.

4.4. Reaction Mechanisms on the Triplet Surface. As stated above, the spin transition at ^{5}**B1** from a quintet ground spin state to the adjacent triplet surface is facilitated by presenting an MECP $^{5-3}$**CP2** between quintet and triplet surfaces. Therefore, the formation of the triplet methylacetylene adducts will be first discussed in this section. The following reaction on the triplet surface is thus described with a consideration of two competing reaction mechanisms. The reactivity and regioselectivity for the triplet pathways are examined by the TOFs calculated using the energetic span model.

4.4.1. The Triplet Chromium Adducts. Unlike the formation of a chromium adduct with a π-coordinated methylacetylene on the quintet surface, a methyl-chromacyclopropene species ^{3}**B** was formed immediately after the spin transition at $^{5-3}$**CP2**. As shown in Figure 5, ^{3}**B** exhibits a C_s symmetry and the 3-

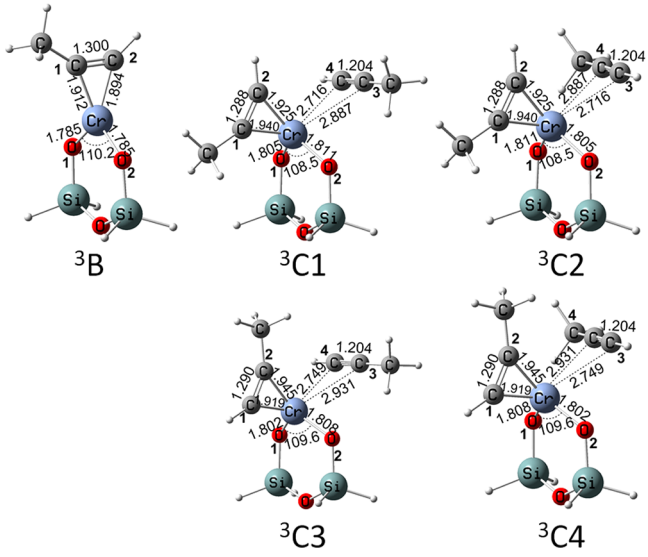

Figure 5. Optimized geometries of the triplet chromium-(methylacetylene)$_n$ (n = 1−2) complexes. Bond lengths are in angstroms. Angles are in degrees.

membered ring in ^{3}**B** lies perpendicular to the $-O_{(1)}-Cr-O_{(2)}-$ model plane with the $Cr-C_{(2)}$ distance of 1.894 Å indicative of the formation of the metal−carbon σ bond. The bond length of the $Cr-C_{(1)}$ is slightly elongated to 1.912 Å due to the steric hindrance of the methyl group. In ^{3}**B**, the triple bond character in the methylacetylene molecule was destroyed and the $C_{(1)}-C_{(2)}$ distance of 1.300 Å showed the formation of a double bond in the 3-membered ring. The coordination of a second methylacetylene molecule on a C_s symmetric ^{3}**B** generates two pairs of enantiomers (^{3}**C1**/^{3}**C2** and ^{3}**C3**/^{3}**C4**). The second methylacetylene molecule could only be weakly coordinated on the chromium center as indicated by the $Cr-C_{(3)}$/$Cr-C_{(4)}$ distance of 2.887 Å/2.716 Å in ^{3}**C1** and 2.931 Å/2.749 Å in ^{3}**C3**, respectively.

4.4.2. Triplet Pathways for Methylacetylene Cyclotrimerization. Expansion of the 3-membered chromacycle in the ^{3}**C** structures from the preceding section may take place in a single step by insertion of one of the methylacetylene ligands coordinated to chromium. This gives rise to four isomers of dimethyl chromacyclopentadiene, namely, ^{3}**F1** (1,3-dimethyl-chromacyclopentadiene), ^{3}**F2** (1,4-dimethyl-chromacyclopentadiene), ^{3}**F3** (2,3-dimethyl-chromacyclopentadiene), and ^{3}**F4** (2,4-dimethyl-chromacyclopentadiene), as drawn in Scheme 3.

All the triplet dimethyl-chromacyclopentadiene species are C_s symmetric and the diene part in ^{3}**F**s forms an absolute planar ring. Similar to that on the quintet surface, ten isomers of ^{3}**H** were generated through the adsorption of a third methylacetylene molecule in two different orientations. For example, the third methylacetylene molecule adsorbed on ^{3}**F1** in a MG-down orientation generates ^{3}**H1Dh** through the formation of a hydrogen bond. Alternatively, a hydrogen-bonded complex ^{3}**H1Uh** was formed by adsorbing a third methylacetylene molecule on ^{3}**F1** in a MG-up orientation. The direct interaction between the chromium center and the third methylacetylene molecule is sterically inhibited by the planar diene part. Interestingly, the cyclic product 1,2,4-TMB could be directly generated from ^{3}**H1Dh** through an intermolecular [4 + 2] cycloaddition. Similarly, for the other three constitutional isomers of ^{3}**H1Dh**, the [4 + 2] cycloaddition takes place in one

dx.doi.org/10.1021/cs400129g | ACS Catal. 2013, 3, 1172−1183

Scheme 3. The Plausible Paths for the Cyclotrimerization of Methylacetylene on the Triplet Surface

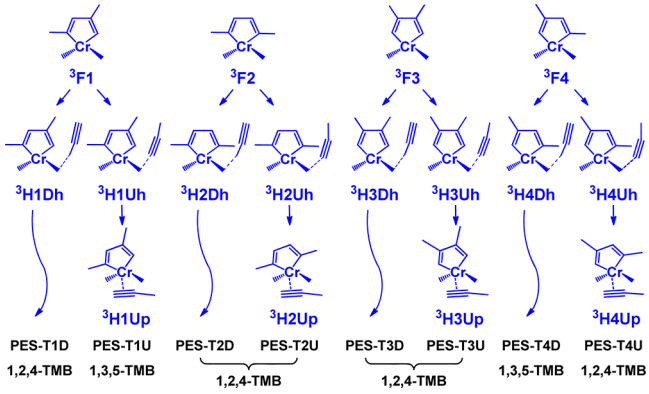

step from the complexes ^{3}**H2Dh**, ^{3}**H3Dh**, and ^{3}**H4Dh**, respectively. However, a thermal transformation is required to break the planarity of the diene ring in ^{3}**H1Uh**, ^{3}**H2Uh**, ^{3}**H3Uh**, and ^{3}**H4Uh**, which transforms the complex ^{3}**H1Uh**−^{3}**H4Uh** with a hydrogen bonded methylacetylene into a π-coordinated complex ^{3}**H1Up**−^{3}**H4Up**. As shown in Scheme 3, there are also six paths leading to the production of 1,2,4-TMB, while two paths generate 1,3,5-TMB. The first pathway PES-T1D will be first discussed in detail, and then the feasibility of all the possible pathways on the triplet surface will be examined by their TOFs.

4.4.3. The Triplet Reaction Pathway (PES-T1D) to 1,2,4-TMB. Following either an intermolecular [4 + 2] cycloaddition pathway (PES-T1Da) or an insertion and reductive elimination pathway (PES-T1Db), the catalytic cycle on the PES-T1D yields the same cyclic product 1,2,4-TMB, as drawn in Scheme 4. The key intermediate ^{3}**F1** is formed through direct insertion

Scheme 4. Mechanisms for Cyclotrimerization of Methylacetylene on the PES-T1D

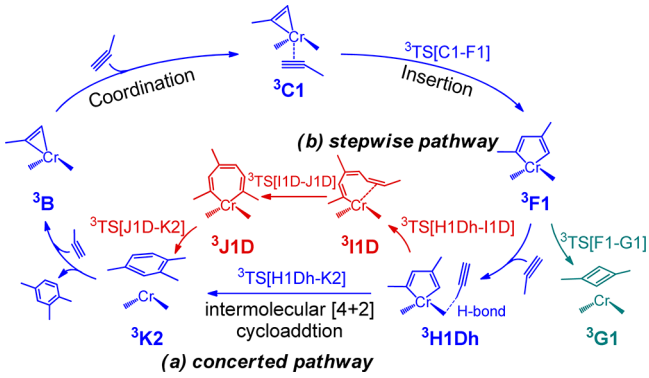

of a second methylacetylene into the 3-membered ring in ^{3}**C1**, which is different from the spontaneous oxidative coupling reaction on the quintet surface. A reductive elimination on ^{3}**F1** generates a dimerization product ^{3}**G1**. Alternatively, ^{3}**H1Dh** is produced by adsorbing a third methylacetylene molecule in a MG-down orientation through the formation of a hydrogen bond. The cyclic product ^{3}**K2** could be generated in a concerted pathway PES-T1Da, or following a stepwise pathway via a 1,3,6-trimethyl-chromacycloheptatriene species ^{3}**J1D**. The first catalytic cycle is then finished through the displacement of the 1,2,4-TMB in the complex ^{3}**K2** by a methylacetylene molecule. After the thermal replacement, a more stable complex ^{3}**B** is regenerated by releasing a free 1,2,4-TMB arene and is ready for the next turn of the catalytic cycle.

The triplet Gibbs free energy profile of the methylacetylene cyclotrimerization catalyzed by the Cr(II)/SiO_2 cluster model is depicted in Figure 6, while the geometrical features of the corresponding species are drawn in Figure 7. The 3-membered ring in the C_s symmetric complex ^{3}**B** showed a bent conformation when a second methylacetylene approached to the chromium center. The coordination of the second methylacetylene on ^{3}**B** generates a methyl-chromacyclopropene(methylacetylene) species ^{3}**C1** with an endergonicity of 6.7 kcal/mol. On the triplet surface, the ring expansion through insertion of the second methylacetylene into the 3-membered ring proceeds via a transition state ^{3}**TS**[**C1-F1**] with a Gibbs free energy barrier of 5.7 kcal/mol. This is an exergonic process by 26.5 kcal/mol. In the ground spin state of ^{3}**F1**, the diene part was formed in an absolute planar metallacyclic 5-membered ring, which is perpendicular to the $-O_{(1)}-Cr-O_{(2)}-$ plane. ^{3}**F1** is a nonaromatic species as indicated by a clear π-localization with $C_{(1)}-C_{(2)}$ and $C_{(3)}-C_{(4)}$ bond lengths of 1.338 Å and 1.343 Å, respectively. The reductive cyclization of ^{3}**F1** to generate a 1,3-dimethyl-cyclobutadiene coordinated species ^{3}**G1** is predicted to be prohibitive by the presence of a high Gibbs free energy barrier of 26.6 kcal/mol.

Alternatively, a third methylacetylene could be adsorbed on ^{3}**F1** in a MG-down orientation yielding a complex ^{3}**H1Dh** through the formation of a weak hydrogen bond of 3.079 Å. This process requires Gibbs free energy of 4.0 kcal/mol. The cyclic product 1,2,4-TMB could be produced in two different ways: (a) a concerted one-step pathway and (b) a stepwise pathway via a 1,3,6-trimethyl-chromacycloheptatriene species ^{3}**J1D**. The first path is an intermolecular [4 + 2] cycloaddition to generate ^{3}**K2** in a single step with a Gibbs free energy barrier of 19.7 kcal/mol. The other path follows in a multistep reaction, which is similar to that on the quintet surface. However, the trimethyl-chromacycloheptatriene is needed to finish the cyclization, which is absent on the quintet surface. This stepwise pathway is disfavored by showing a transition state ^{3}**TS**[**H1Dh-I1D**], which is higher in Gibbs free energy by 2.2 kcal/mol than that of the transition state ^{3}**TS**[**H1Dh-K2**] for the intermolecular [4 + 2] cycloaddition. As will be discussed in the next section, this amount of energy difference results in a TOF of 0.093 h^{-1} for [4 + 2] cycloaddition reaction pathway PES-T1Da, which is about 40 times larger than the TOF for the stepwise reaction pathway PES-T1Db of 0.0023 h^{-1}.

On the Gibbs free energy profiles of the PES-T1D, there are three key transition states that determine the reactivity of three different pathways. The first path is to generate a dimerization product via a transition state ^{3}**TS**[**F1-G1**] with a free energy barrier of 26.6 kcal/mol, which is higher in Gibbs free energy by 2.9 kcal/mol than that required to finish a [4 + 2] cycloaddition. Therefore, the intermolecular [4 + 2] cyclo-addition is the most favorable pathway to produce 1,2,4-TMB on the PES-T1D. The regioselectivity and reactivity for all the reaction pathways on the triplet surface will be discussed in the following subsection.

4.4.4. Reactivity and Regioselectivity for the Triplet Pathways. The coordination of an unsymmetrical molecule in a different orientation plays a key role in determining the

dx.doi.org/10.1021/cs400129g | ACS Catal. 2013, 3, 1172−1183

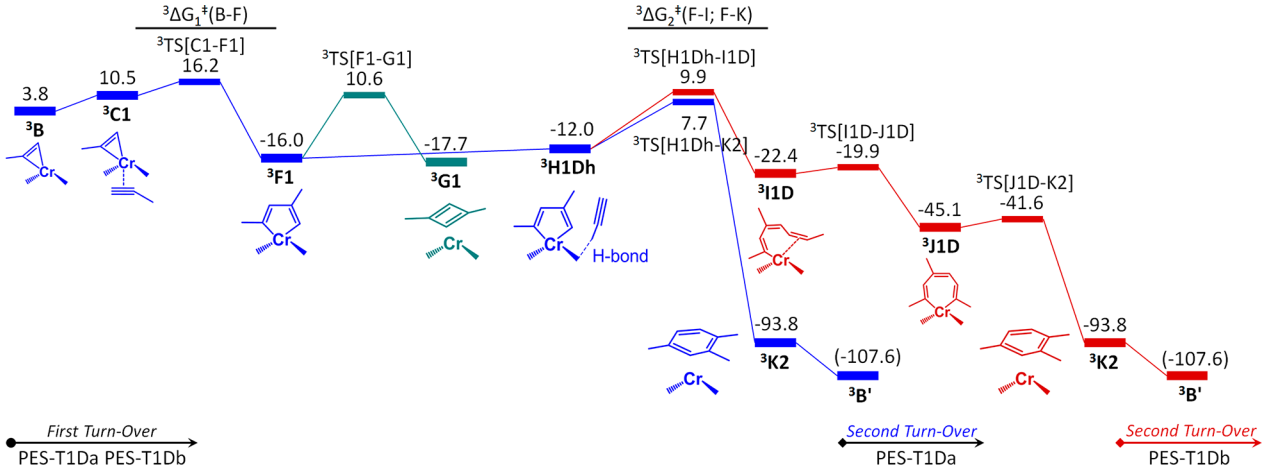

Figure 6. Gibbs free energy profile at 298.15 K of the triplet reaction pathway (PES-T1D) for methylacetylene cyclotrimerization over the Cr(II)/SiO_2 cluster model. The reaction pathway via intermolecular [4 + 2] cycloaddition is depicted in blue, while the stepwise pathway is in dark red. The reaction to generate 1,3-dimethyle-cyclobutadiene ^{3}**G1** is in dark teal. Energies are in kcal/mol and relative to ^{5}**A** plus the corresponding number of methylacetylenes.

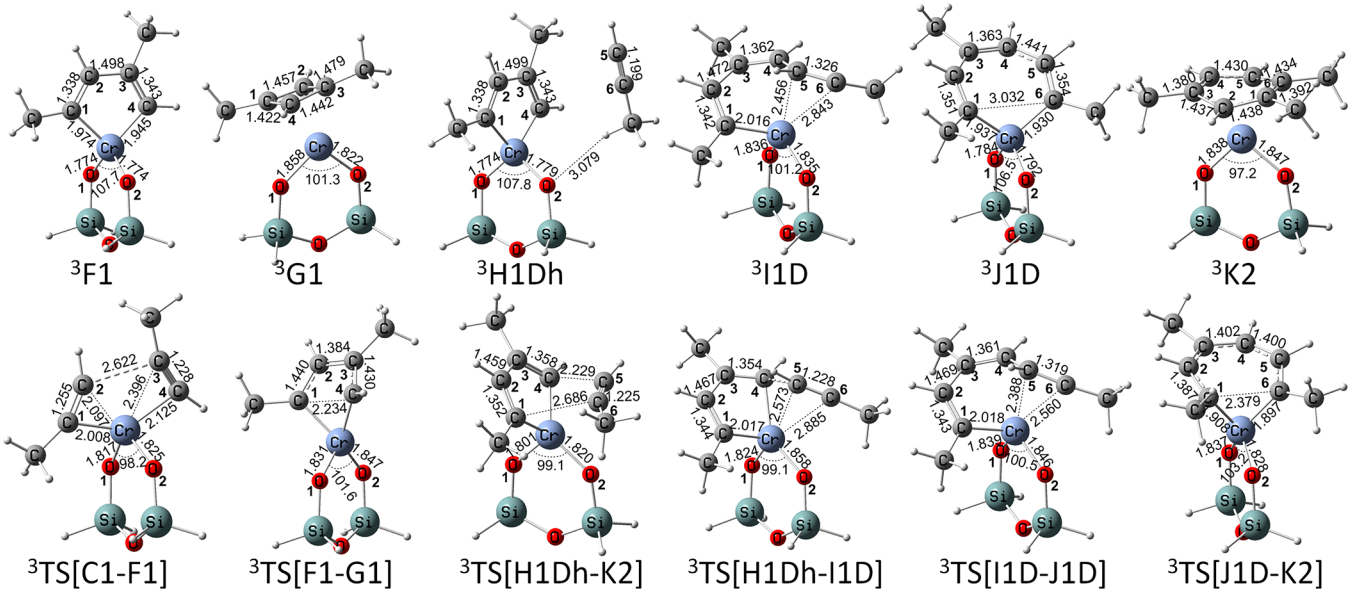

Figure 7. Optimized geometries of the structures on the PES-T1D for methylacetylene cyclotrimerization over the Cr(II)/SiO_2 cluster model. Bond lengths are in angstroms. Angles are in degrees.

regioselectivities of the cycloaddition products. When a methylacetylene molecule being adsorbed on each of the four constitutional isomers ^{3}**F1**−^{3}**F4** through the formation of a hydrogen bond, two regioisomeric chromium(methylacetylene) adducts could be generated. As shown in Scheme 5, for instance, the hydrogen-bonded complex ^{3}**H1Dh** is produced by adsorbing a methylacetylene molecule on ^{3}**F1** in a MG-down orientation, while the MG-up adsorption of a methylacetylene generates another product, ^{3}**H1Uh**. The adducts ^{3}**H3Dh** and ^{3}**H3Uh** were generated in the same manner by adsorbing a methylacetylene on ^{3}**F3**. These two complexes ^{3}**H1Dh** and ^{3}**H3Dh** showed a similar reaction behavior. The following two paths including one-step [4 + 2] cycloaddition and the insertion followed by a reductive elimination pathway proceeded directly from the same complex ^{3}**H1Dh** or ^{3}**H3Dh**, as confirmed by the full IRC calculations (the IRC trajectories of the PES-T1D, see Figure S6 in the Supporting Information). However, for the complexes ^{3}**H1Uh**/^{3}**H3Uh**, a different reaction pathway was obtained following the direction of the IRC trajectories. A thermal transformation of ^{3}**H1Uh**/^{3}**H3Uh** is required for both of these two paths to generate the cyclic product. After the transformation, a π-complex ^{3}**H1Up**/^{3}**H3Up** was generated with a distorted diene ring and a methylacetylene coordinated on the chromium center directly. For the adsorption of a methylacetylene molecule in MG-down orientation on ^{3}**F2**/^{3}**F4**, two kinds of complexes ^{3}**H2Dh**/^{3}**H4Dh** and ^{3}**H2Dh′**/^{3}**H4Dh′**, could be located. The following concerted [4 + 2] cycloaddition takes place at ^{3}**H2Dh**/^{3}**H4Dh**, while the stepwise pathway occurs at ^{3}**H2Dh′**/^{3}**H4Dh′**. The adsorption of a methylacetylene molecule in MG-up orientation on ^{3}**F2** and ^{3}**F4** generated another two complexes, ^{3}**H2Uh** and ^{3}**H4Uh**, respectively. The reaction behavior of ^{3}**H2Uh**/^{3}**H4Uh** is also different from that of ^{3}**H1Uh**/^{3}**H3Uh**. For the [4 + 2] cycloaddition pathway, a thermal transformation of ^{3}**H2Uh**/^{3}**H4Uh** to a π-coordination complex ^{3}**H2Up**/^{3}**H4Up** is still necessary to finish the

dx.doi.org/10.1021/cs400129g | ACS Catal. 2013, 3, 1172−1183

Scheme 5. Various Reaction Pathways for Cyclotrimerization of Methylacetylene on the Triplet Surface[a]

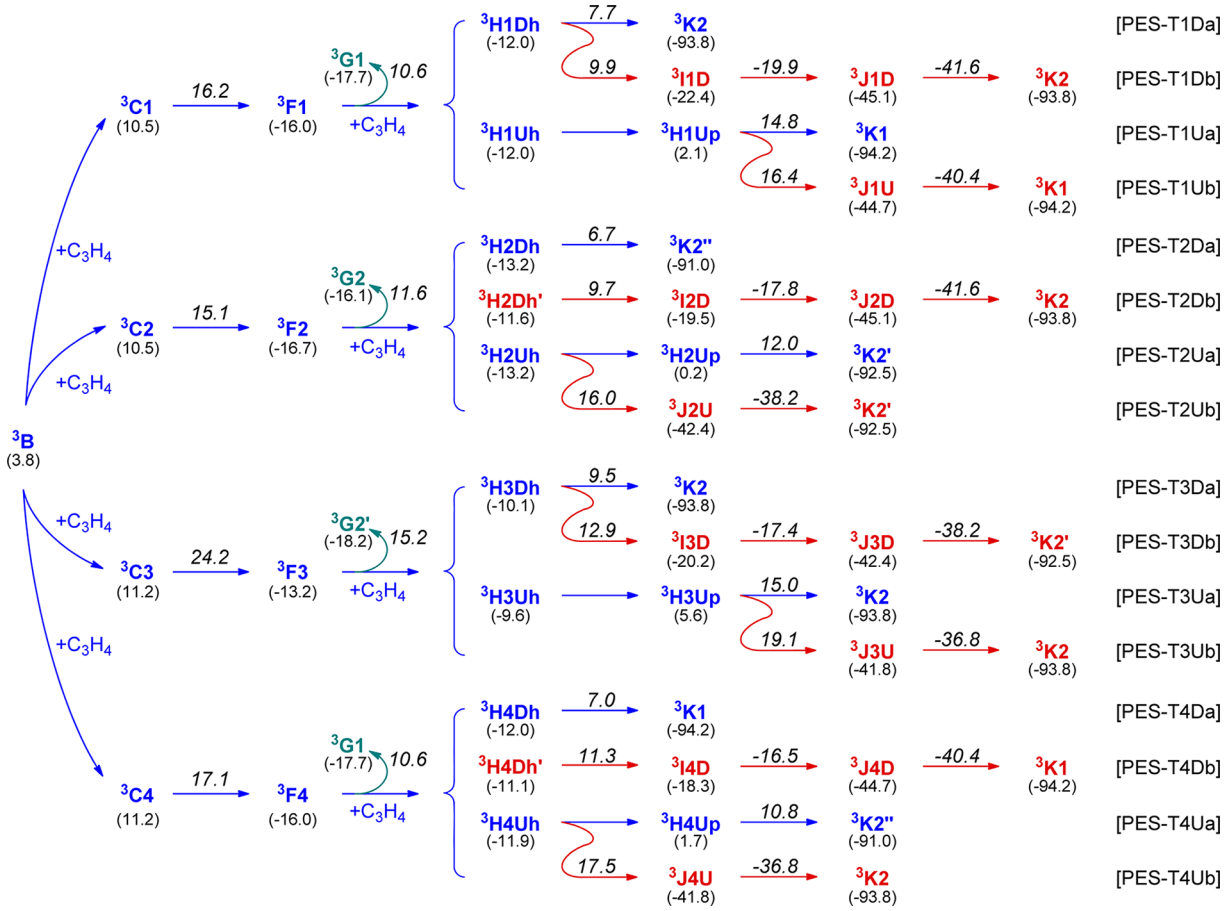

[a]The reaction pathways via intermolecular [4 + 2] cycloaddition are depicted in blue, while the stepwise pathways are in dark red. The Gibbs free energies for the intermediates are listed in parentheses, and the Gibbs free energies for the transition states are shown above the arrow. Energies are in kcal/mol and relative to ^{5}**A** plus the corresponding number of methylacetylenes.

cyclization. However, a 7-memerbed ring was directly generated from ^{3}**H2Uh**/^{3}**H4Uh** by insertion of the methylacetylene into the dimethyl-chromacyclopentadiene species on the stepwise pathways.

The relative Gibbs free energies for all the intermediates are listed in parentheses below the labels, while the relative free energies for the transition states are given above the arrow, as shown in Scheme 5. The reactivity and regioselectivity for all 16 reaction pathways are discussed below. The calculated TOFs for all 16 pathways are given in Table 3.

On the quintet surface, the reaction is inhibited by the spontaneous oxidative coupling of the two coordinated methylacetylene molecules. However, a methyl-chromacyclopropene species ^{3}**B** was formed immediately after the spin flipping via $^{5-3}$**CP2**. The following insertion of the second methylacetylene into the 3-membered ring is predicted to be a fast reaction. The activation barrier for this process is noted as $^3\Delta G_1^{\ddagger}$, which represents the free energy difference between the transition state ^{3}**TS**[**C-F**] and the most stable complex ^{3}**B**. ^{3}**TS**[**H-K**] is the rate-determining transition state on the concerted pathway a, while ^{3}**TS**[**H-I**] determines the reactivity of the stepwise pathway b. Both of these two transition states are rate-determining, and the activation barrier required for these transformations is referred to as $^3\Delta G_2^{\ddagger}$. In general, the difference of 2 kcal/mol in free-energy barrier would result in a difference of TOF by about 1−2 orders of magnitude. As listed in Table 3, the TOF for each concerted [4 + 2] cycloaddition pathway a is around 15 to 10^5 times larger than its competitive stepwise pathway b with a free energy difference $^3\Delta G_2^{\ddagger}$(b) − $^3\Delta G_2^{\ddagger}$(a) of 1.6 to 6.7 kcal/mol. The calculated TOFs at 298.15 K for the [4 + 2] cycloaddition pathways PES-T1Da, PES-T2Da, PES-T3Da, and PES-T4Da are 0.093 h^{-1}, 0.16 h^{-1}, 0.50 h^{-1}, and 0.30 h^{-1}, respectively. (IRC trajectories: see Figure S7 in the Supporting Information.) However, the reactivity for the other four [4 + 2] cycloaddition pathways PES-T1Ua, PES-T2Ua, PES-T3Ua, and PES-T4Ua are negligible when compared with that of the four pathways (PES-T(1−4)Da). Actually, for the reaction pathways PES-T1Ua, PES-T2Ua, PES-T3Ua, and PES-T4Ua, the chromacyclopentadiene(methylacetylene) complexes (^{3}**H1Uh**−^{3}**H4Uh**) with a third methylacetylene adsorbed on the cluster model through hydrogen bonding in a MG-up orientation could not go to a direct [4 + 2] cycloaddition. A thermal transformation of the hydrogen-bonded complex (^{3}**H1Uh**−^{3}**H4Uh**) to a π-coordination complex (^{3}**H1Up**−^{3}**H4Up**) is needed to finish the cyclization, and a slightly higher activation barrier is required for the consequent [4 + 2] cycloaddition. This finding suggests that the third methylacetylene molecule prefers an adsorption on ^{3}**Fs** in a MG-down orientation. As a result, the cyclotrimerization of methylacetylene on the triplet surface is predicted to be a direct [4 + 2] cycloaddition via four different pathways PES-T1Da,

dx.doi.org/10.1021/cs400129g | ACS Catal. 2013, 3, 1172−1183

Table 3. The Gibbs Free Energy Barriers and the Calculated TOFs on Each of the Triplet Pathways[a] for the Cyclotrimerization of Methylacetylene into TMB

pathway	$^3\Delta G_1^{\ddagger}$	$^3\Delta G_2^{\ddagger}$	TOF
PES-T1D			
a	12.4	23.7	0.093
b	12.4	25.9	0.0023
PES-T1U			
a	12.4	30.8	5.9×10^{-7}
b	12.4	32.4	4.0×10^{-8}
PES-T2D			
a	11.3	23.4	0.16
b	11.3	26.4	0.0010
PES-T2U			
a	11.3	28.7	2.1×10^{-5}
b	11.3	32.7	2.4×10^{-8}
PES-T3D			
a	20.4	22.7	0.50
b	20.4	26.1	0.0016
PES-T3U			
a	20.4	28.2	4.8×10^{-5}
b	20.4	32.3	4.7×10^{-8}
PES-T4D			
a	13.3	23.7	0.30
b	13.3	27.3	0.00022
PES-T4U			
a	13.3	26.8	5.1×10^{-4}
b	13.3	33.5	6.2×10^{-9}

[a]The intermolecular [4 + 2] cycloaddition path is shown as pathway a. The stepwise reaction pathway is shown as pathway b. Energies are in kcal/mol. TOFs are in hour^{-1}.

PES-T2Da, PES-T3Da, and PES-T4Da. One pathway PES-T4Da leads to production of 1,3,5-TMB, while the other three pathways generate 1,2,4-TMB. It is worthy of note that the calculated $\langle S^2 \rangle$ values differ from $S(S + 1)$ by less than 10% for all the species on these four reaction pathways. A detailed discussion for the other species is given in section S5 in the Supporting Information (Figure S8 and Tables S2 and S3).

4.5. Effects of Temperature and Silica Support. When the most plausible reaction pathways are recognized, it is particularly interesting to analyze how the TOF changes at these two experimental conditions: (a) at 250 K and 1 atm[16] and (b) at 363 K and 40.8 atm.[15] All the calculated TOFs are listed in Table 4, and the corresponding Gibbs free energies are given in Table S4 in the Supporting Information. As shown in Table 4, the temperature affects the magnitude of the TOF enormously with a slightly different selectivity between 1,3,5-TMB and 1,2,4-TMB. The ratio of the TOF for producing 1,3,5-TMB and 1,2,4-TMB is 0.48 at 363 K, which is larger than the experimental value of 0.18.[15] Because the real Phillips chromium catalyst is supported on the silica surface, we further studied the most plausible reaction pathways using a large model *silica*-A, as graphically shown in Figure 1. The TOF for each of the reaction pathways increased by a factor 9−17 at 250 K, 5.3−8.6 at 298.15 K, and 3.9−7.3 at 363 K, respectively. For instance, the TOFs calculated at 363 K using the six-membered cluster model A for the [4 + 2] cycloaddition pathways PES-T1Da, PES-T2Da, PES-T3Da, and PES-T4Da are 140 h^{-1}, 170 h^{-1}, 440 h^{-1}, and 360 h^{-1}, respectively. When using the extended model *silica*-A, the calculated TOFs increased to 570 h^{-1}, 670 h^{-1}, 3200 h^{-1}, and 1700 h^{-1}, respectively. Interestingly, the ratio of 1,3,5-TMB to 1,2,4-TMB in the product decreased at all three conditions, indicating that 1,2,4-TMB is a major product on a silica supported active site. Moreover, the dispersion corrections are considered for all the silica supported species and the TOFs calculated using the corrected Gibbs free energies are also given in Table 4. Since the transition states ^{3}**TS**[**C-F**]$_{1-4}$ and ^{3}**TS**[**H-K**]$_{1-4}$ are highly stabilized relative to starting materials by dispersion corrections, the corresponding TOFs for all four reaction pathways increased by about 4−8 orders of magnitude calculated at three different conditions. The ratio of 1,3,5-TMB to 1,2,4-TMB decreases to 0.22, 0.22, and 0.32 at 250 K, 298.15 K, and 363 K, respectively. The TOF is extremely sensitive to the calculated Gibbs free energies and depends exponentially on the activation energies. Although the calculated ratio of 1,3,5-TMB to 1,2,4-TMB of 0.32 at 363 K is larger than the experimental value, it is predictive for the selectivity. The 1,2,4-TMB is preferred as a dominant product for the cyclotrimerization of the methylacetylene catalyzed by the Phillips Cr/silica catalyst. It is worthy of note that the titanium catalyzed methylacetylene cyclotrimerization gives a similar ratio of 0.33 of 1,3,5-TMB to1,2,4-TMB.[59]

4.6. The Formation of the First Chromium−Carbon Bond. There is a long-standing question for the Phillips Cr/silica catalyst: how the first chromium−carbon bond is formed without using any organometallic cocatalyst? After reduction of chromium to the divalent state, the model catalyst and all the chromium(alkyne) adducts showed a quintet ground spin state. However, the following reaction on the quintet surface is inhibited by the oxidative coupling of the two coordinated alkynes to yield a 5-membered ring. It is hard for the spin flipping to the triplet surface to occur at the naked chromium(II) in the model catalyst as the MECP $^{5-3}$**CP1** lies much higher in energy. The coordination of an alkyne on the cluster model results in a stable chromium(alkyne) complex, and the spin transition at ^{5}**B1** is predicted to be much more facile at $^{5-3}$**CP2** with a moderate energy barrier. After the spin

Table 4. The TOFs for the Most Plausible Reaction Pathways[a] via an Intermolecular [4 + 2] Cycloaddition of Methylacetylene into TMB

	TOF_{250K} (I/II/III)[b]	$TOF_{298.15K}$ (I/II/III)[b]	TOF_{363K} (I/II/III)[b]	
PES-T1Da	$0.0020/0.022/1.9 \times 10^6$	$0.093/0.60/3.3 \times 10^6$	$140/570/1.0 \times 10^8$	1,2,4-TMB (T1Da, T2Da, T3Da)
PES-T2Da	$0.0037/0.034/4.9 \times 10^6$	$0.16/0.85/6.3 \times 10^6$	$170/670/1.5 \times 10^8$	
PES-T3Da	$0.012/0.20/3.6 \times 10^5$	$0.50/4.3/3.0 \times 10^6$	$440/3200/9.6 \times 10^7$	
PES-T4Da	$0.0082/0.092/1.6 \times 10^6$	$0.30/2.0/2.8 \times 10^6$	$360/1700/1.1 \times 10^8$	1,3,5-TMB
ratio of TOF (1,3,5-/1,2,4-TMB)	0.46/0.36/0.22	0.40/0.35/0.22	0.48/0.38/0.32	

[a]The Gibbs free energy profiles were calculated at 250 K and 1 atm, 298.15 K and 1 atm, and 363 K and 40.8 atm, respectively. [b]TOFs were calculated on the basis of the Gibbs free energies, (I) as computed for the cluster model A, (II) as computed for the extended model *silica*-A, and (III) as computed for the extended model *silica*-A including dispersion corrections. TOFs are in hour^{-1}.

dx.doi.org/10.1021/cs400129g | ACS Catal. 2013, 3, 1172−1183

flipping, the chromium−carbon bond is already formed in triplet ^{3}**B** and the following insertion of a second alkyne can proceed easily. Therefore, the chromium−carbon bond could not be formed on the quintet surface, but is formed immediately after the spin flipping to the triplet surface at the chromium(alkyne) complex.

5. CONCLUSIONS

In this work, the mechanisms of methylacetylene cyclotrimerization over a six-membered chromasiloxane(II) ring cluster model and a silica supported cluster model for the Phillips Cr(II)/silica catalyst have been investigated through a detailed DFT study. Twenty-one kinds of chromium-(methylacetylene)$_n$ (n = 1−3) complexes have been successfully optimized on the quintet surface. The chromium-(methylacetylene) complexes ^{5}**B1** and ^{5}**B2** are more stable than the adducts with two coordinated methylacetylenes (^{5}**C1**, ^{5}**C2**, ^{5}**C3**, and ^{5}**C4**). The third methylacetylene molecule could only be adsorbed on the cluster model through the formation of a hydrogen bond. All 15 kinds of chromium-(methylacetylene)$_3$ adducts are not stable at room temperature.

On the quintet surface, the methylacetylene cyclotrimerization is inhibited by the oxidative coupling of two coordinated methylacetylenes to generate a dimethyl-chromacyclopentadiene species. This step requires an activation barrier of about 40 kcal/mol in Gibbs free energy. Thus the TOFs for the quintet reaction pathways are extremely small. The reactivity was raised after a spin flipping to the triplet surface at the most stable chromium(methylacetylene) complex ^{5}**B1**. After the spin flipping reaction, a methyl-chromacyclopropene species was formed immediately on the triplet surface. The TOF for each concerted [4 + 2] cycloaddition pathway (a) is much larger than its competitive stepwise pathway (b), which rules out all eight stepwise pathways. Four pathways PES-T1Da, PES-T2Da, PES-T3Da, and PES-T4Da via a chromacyclopentadiene-(methylacetylene) complex (^{3}**H1Dh**−^{3}**H4Dh**) with a third methylacetylene adsorbed on the cluster model through hydrogen bonding in a MG-down orientation showed a higher reactivity for methylacetylene cyclotrimerization. The PES-T4Da leads to the production of 1,3,5-trimethylbenzene, while the other three pathways generate 1,2,4-trimethylbenzene. With a consideration of the effects of the silica support and inclusion of the dispersion correction in the final calculated energies, the ratio of the 1,3,5- to 1,2,4-TMB is 0.32 at 363 K, predicting that the 1,2,4-TMB is the dominant product in the cyclotrimerization of methylacetylene catalyzed by the Phillips Cr/silica catalyst.

■ ASSOCIATED CONTENT

Ⓢ Supporting Information

The optimized geometries for the Cr(II)/SiO_2·$(C_3H_4)_3$ complexes. A detailed discussion of the mechanisms for methylacetylene cyclotrimerization catalyzed by Cr/SiO_2 cluster model on the quintet surface. The relative energies for the key intermediates under three different spin sates including singlet, triplet, and quintet. Quintet IRC trajectories. Spin contaminations analysis for the key transition states on the quintet and triplet surfaces. The Cartesian coordinates, the total energies and Gibbs free energies for all the complexes. This material is available free of charge via the Internet at http://pubs.acs.org.

■ AUTHOR INFORMATION

Corresponding Author

*Fax: 0086-21-64253627. E-mail: boping@ecust.edu.cn.

Notes

The authors declare no competing financial interest.

■ ACKNOWLEDGMENTS

We thank the National Natural Science Foundation of China (20774025), the Program of Introducing Talents of Discipline to Universities (B08021), and the Fundamental Research Funds for the Central Universities for financial support. We thank Prof. J. N. Harvey for the sharing of his remarkable code created for MECP calculation, and Dr. S. Kozuch for sending us the AUTOF program. We thank Prof. S. Grimme for his kind suggestions on the calculation of dispersion corrections.

■ REFERENCES

(1) McDaniel, M. P. *Adv. Catal.* **2010**, *53*, 123−606.
(2) Hogan, J. P.; Banks, R. L. U.S. Patent 2,825,721, March 4, 1958.
(3) Lanning, W. C.; Clark, A.; Bartlesville, O. U.S. Patent 2,819,325, Jan 7, 1958.
(4) Groppo, E.; Lamberti, C.; Bordiga, S.; Spoto, G.; Zecchina, A. *Chem. Rev.* **2005**, *105*, 115−183.
(5) Espelid, O.; Børve, K. J. *J. Catal.* **2000**, *195*, 125−139.
(6) Espelid, O.; Børve, K. J. *J. Catal.* **2002**, *205*, 366−374.
(7) Espelid, O.; Børve, K. J. *J. Catal.* **2002**, *206*, 331−338.
(8) Demmelmaier, C. A.; White, R. E.; van Bokhoven, J. A.; Scott, S. L. *J. Catal.* **2009**, *262*, 44−56.
(9) Damin, A.; Vitillo, J. G.; Ricchiardi, G.; Bordiga, S.; Lamberti, C.; Groppo, E.; Zecchina, A. *J. Phys. Chem. A* **2009**, *113*, 14261−14269.
(10) Cheng, R. H.; Xu, C.; Liu, Z.; Dong, Q.; He, X. L.; Fang, Y. W.; Terano, M.; Hu, Y.; Pullukat, T. J.; Liu, B. P. *J. Catal.* **2010**, *273*, 103−115.
(11) Gianolio, D.; Groppo, E.; Vitillo, J. G.; Damin, A.; Bordiga, S.; Zecchina, A.; Lamberti, C. *Chem. Commun.* **2010**, *46*, 976−978.
(12) Liu, Z.; Cheng, R.; He, X.; Wu, X.; Liu, B. *J. Phys. Chem. A* **2012**, *116*, 7538−7549.
(13) Zhong, L.; Lee, M.-Y.; Liu, Z.; Wanglee, Y.-J.; Liu, B.; Scott, S. L. *J. Catal.* **2012**, *293*, 1−12.
(14) Zhong, L.; Liu, Z.; Cheng, R.; Tang, S.; Qiu, P.; He, X.; Terano, M.; Liu, B. *ChemCatChem* **2012**, *4*, 872−881.
(15) Clark, A.; Hogan, J. P.; Witt, D. R.; Lanning, W. C. *Proc. World Pet. Congr.* **1959**, *4*, 267−273.
(16) Zecchina, A.; Bertarione, S.; Damin, A.; Scarano, D.; Lamberti, C.; Prestipino, C.; Spoto, G.; Bordiga, S. *Phys. Chem. Chem. Phys.* **2003**, *5*, 4414−4417.
(17) Hardesty, J. H.; Koerner, J. B.; Albright, T. A.; Lee, G.-Y. *J. Am. Chem. Soc.* **1999**, *121*, 6055−6067.
(18) Abbet, S.; Sanchez, A.; Heiz, U.; Schneider, W. D.; Ferrari, A. M.; Pacchioni, G.; Roesch, N. *J. Am. Chem. Soc.* **2000**, *122*, 3453−3457.
(19) Ferrari, A. M.; Giordano, L.; Roesch, N.; Heiz, U.; Abbet, S.; Sanchez, A.; Pacchioni, G. *J. Phys. Chem. B* **2000**, *104*, 10612−10617.
(20) Kirchner, K.; Calhorda, M. J.; Schmid, R.; Veiros, L. F. *J. Am. Chem. Soc.* **2003**, *125*, 11721−11729.
(21) Dahy, A. A.; Koga, N. *Bull. Chem. Soc. Jpn.* **2005**, *78*, 781−791.
(22) Dahy, A. A.; Suresh, C. H.; Koga, N. *Bull. Chem. Soc. Jpn.* **2005**, *78*, 792−803.
(23) Martinez, M.; Michelini, M. D. C.; Rivalta, I.; Russo, N.; Sicilia, E. *Inorg. Chem.* **2005**, *44*, 9807−9816.
(24) Gandon, V.; Agenet, N.; Vollhardt, K. P. C.; Malacria, M.; Aubert, C. *J. Am. Chem. Soc.* **2006**, *128*, 8509−8520.
(25) Kletnieks, P. W.; Liang, A. J.; Craciun, R.; Ehresmann, J. O.; Marcus, D. M.; Bhirud, V. A.; Klaric, M. M.; Haymann, M. J.; Guenther, D. R.; Bagatchenko, O. P.; Dixon, D. A.; Gates, B. C.; Haw, J. F. *Chem.—Eur. J.* **2007**, *13*, 7294−7304.

(26) Orian, L.; Van Stralen, J. N. P.; Bickelhaupt, F. M. *Organometallics* **2007**, *26*, 3816−3830.
(27) Ma, Y. P.; Xue, W.; Wang, Z. C.; Ge, M. F.; He, S. G. *J. Phys. Chem. A* **2008**, *112*, 3731−3741.
(28) Varela, J. A.; Rubin, S. G.; Castedo, L.; Saa, C. *J. Org. Chem.* **2008**, *73*, 1320−1332.
(29) Xu, R.; Winget, P.; Clark, T. *Eur. J. Inorg. Chem.* **2008**, 2874−2883.
(30) Dahy, A. A.; Yamada, K.; Koga, N. *Organometallics* **2009**, *28*, 3636−3649.
(31) Dachs, A.; Osuna, S.; Roglans, A.; Sola, M. *Organometallics* **2010**, *29*, 562−569.
(32) Calhorda, M. J.; Costa, P. J.; Kirchner, K. A. *Inorg. Chim. Acta* **2011**, *374*, 24−35.
(33) Kozuch, S.; Shaik, S. *J. Am. Chem. Soc.* **2006**, *128*, 3355−3365.
(34) Kozuch, S.; Shaik, S. *J. Phys. Chem. A* **2008**, *112*, 6032−6041.
(35) Uhe, A.; Kozuch, S.; Shaik, S. *J. Comput. Chem.* **2011**, *32*, 978−985.
(36) Kozuch, S.; Shaik, S. *Acc. Chem. Res.* **2011**, *44*, 101−110.
(37) Kozuch, S. *WIREs Comput. Mol. Sci.* **2012**, *2*, 795−815.
(38) Sautet, P.; Delbecq, F. *Chem. Rev.* **2010**, *110*, 1788−1806.
(39) Chuang, I. S.; Kinney, D. R.; Bronnimann, C. E.; Zeigler, R. C.; Maciel, G. E. *J. Phys. Chem.* **1992**, *96*, 4027−4034.
(40) Chuang, I. S.; Maciel, G. E. *J. Am. Chem. Soc.* **1996**, *118*, 401−406.
(41) Chuang, I. S.; Maciel, G. E. *J. Phys. Chem. B* **1997**, *101*, 3052−3064.
(42) Sindorf, D. W.; Maciel, G. E. *J. Am. Chem. Soc.* **1983**, *105*, 1487−1493.
(43) Branda, M. M.; Castellani, N. J. *Surf. Sci.* **1997**, *393*, 171−178.
(44) Vigné-Maeder, F.; Sautet, P. *J. Phys. Chem. B* **1997**, *101*, 8197−8203.
(45) Mortensen, J. J.; Parrinello, M. *J. Phys. Chem. B* **2000**, *104*, 2901−2907.
(46) Khaliullin, R. Z.; Bell, A. T. *J. Phys. Chem. B* **2002**, *106*, 7832−7838.
(47) Handzlik, J. *J. Phys. Chem. B* **2005**, *109*, 20794−20804.
(48) Solans-Monfort, X.; Filhol, J.-S.; Coperet, C.; Eisenstein, O. *New J. Chem.* **2006**, *30*, 842−850.
(49) Handzlik, J. *J. Phys. Chem. C* **2007**, *111*, 9337−9348.
(50) Handzlik, J. *Int. J. Quantum Chem.* **2007**, *107*, 2111−2119.
(51) Handzlik, J.; Ogonowski, J. *J. Phys. Chem. C* **2012**, *116*, 5571−5584.
(52) Frisch, M. J.; Trucks, G. W.; Schlegel, H. B.; Scuseria, G. E.; Robb, M. A.; Cheeseman, J. R.; Scalmani, G.; Barone, V.; Mennucci, B.; Petersson, G. A.; Nakatsuji, H.; Caricato, M.; Li, X.; Hratchian, H. P.; Izmaylov, A. F.; Bloino, J.; Zheng, G.; Sonnenberg, J. L.; Hada, M.; Ehara, M.; Toyota, K.; Fukuda, R.; Hasegawa, J.; Ishida, M.; Nakajima, T.; Honda, Y.; Kitao, O.; Nakai, H.; Vreven, T.; Montgomery, J. A., Jr.; Peralta, J. E.; Ogliaro, F.; Bearpark, M.; Heyd, J. J.; Brothers, E.; Kudin, K. N.; Staroverov, V. N.; Kobayashi, R.; Normand, J.; Raghavachari, K.; Rendell, A.; Burant, J. C.; Iyengar, S. S.; Tomasi, J.; Cossi, M.; Rega, N.; Millam, J. M.; Klene, M.; Knox, J. E.; Cross, J. B.; Bakken, V.; Adamo, C.; Jaramillo, J.; Gomperts, R.; Stratmann, R. E.; Yazyev, O.; Austin, A. J.; Cammi, R.; Pomelli, C.; Ochterski, J. W.; Martin, R. L.; Morokuma, K.; Zakrzewski, V. G.; Voth, G. A.; Salvador, P.; Dannenberg, J. J.; Dapprich, S.; Daniels, A. D.; Farkas, O.; Foresman, J. B.; Ortiz, J. V.; Cioslowski, J.; Fox, D. J. *Gaussian 09, revision A.01*; Gaussian, Inc.: Wallingford, CT, 2009.
(53) Harvey, J. N.; Aschi, M.; Schwarz, H.; Koch, W. *Theor. Chem. Acc.* **1998**, *99*, 95−99.
(54) Harvey, J. N.; Aschi, M. *Phys. Chem. Chem. Phys.* **1999**, *1*, 5555−5563.
(55) Grimme, S.; Antony, J.; Ehrlich, S.; Krieg, H. *J. Chem. Phys.* **2010**, *132*, 154104(1−19).
(56) http://toc.uni-muenster.de/DFTD3/.
(57) Liu, Z.; Zhong, L.; Yang, Y.; Cheng, R.; Liu, B. *J. Phys. Chem. A* **2011**, *115*, 8131−8141.
(58) Yang, Y.; Liu, Z.; Zhong, L.; Qiu, P.; Dong, Q.; Cheng, R.; Vanderbilt, J.; Liu, B. *Organometallics* **2011**, *30*, 5297−5302.
(59) Pierce, K. G.; Barteau, M. A. *J. Phys. Chem.* **1994**, *98*, 3882−3892.